Infinite-Q guided modes radiate in the continuum

Kaili Sun,[1] Heng Wei,[2] Weijin Chen,[2] Yang Chen,[3] Yangjian Cai,[1] Cheng-Wei Qiu,[2,*] and Zhanghua Han[1,†]

[1]*Shandong Provincial Key Laboratory of Optics and Photonic Devices, Center of Light Manipulation and Applications, School of Physics and Electronics, Shandong Normal University, Jinan 250358, China*

[2]*Department of Electrical and Computer Engineering, National University of Singapore, Singapore, Singapore 117583*

[3]*Chinese Academy of Sciences Key Laboratory of Mechanical Behavior and Design of Materials, Department of Precision Machinery and Precision Instrumentation, University of Science and Technology of China, Hefei, China*

(Received 23 August 2022; revised 1 January 2023; accepted 3 February 2023; published 15 March 2023)

Guided modes in photonic structures, with broadband infinite-quality factors, are inaccessible from the far field due to the momentum mismatch. They become leaky modes in the continuum when the mismatch is compensated for by introducing periodic perturbations to form photonic structures. However, the quality factors (Q factors) of such leaky modes deteriorate significantly in most regions of the k-space except at a few discrete high-symmetry points. It is an intriguing question as to whether guided modes can hop above the light cone and yet maintain high Q. Here, we propose a double-band-folding strategy to achieve high-Q leaky modes in compound lattices, exemplified with a one-dimensional grating and a two-dimensional zigzag array of dielectric disks. The Q factor of those leaky modes can be made ultrahigh at arbitrarily any incident angles, showing that such modes do not originate from bound states in the continuum (BICs) above the light cone. Our findings provide unique insight for elucidating the relations between guided modes, BICs, quasi-BICs, and radiation. They further provide a generalized recipe for numerous optical applications such as all-dielectric sensing, lasing, and nonlinear generation with multiple inputs.

DOI: 10.1103/PhysRevB.107.115415

The use of resonant photonic structures is at the heart of current nanophotonic research. Ideally, such resonance should be associated with a leaky mode, whose dispersion curve is located above the light cone to facilitate its coupling to and thus excitation by free-space propagating waves. One vital parameter of a leaky resonance is its Q factor, which, although measured by the spectral linewidth in the far field, intrinsically connects many characteristics important for nanoscale light-matter interactions, e.g., the maximum local field enhancement [1], the effective interaction lengths within the same volume, and the local density of optical states (LDOS). The Purcell factor of the resonance, which is proportional to Q/V (V is the mode volume) [2], should be large enough to ensure high local electromagnetic field enhancement. Photonic crystal cavities [3] and whispering-gallery-mode resonators [4], although with superhigh Q factors, are still not ideal due to their relatively large footprint. In this respect, optical nanostructures with tight modal confinement are more attractive. More importantly, given a specific photonic structure, the resonant field enhancement should be accessible in a broad spectral range to be useful for practical applications, where wide spectral tunability or multiple input frequencies are required. Those applications may include nonlinear optics such as sum/difference frequency generation [5], optical switches and tunable optical delays in all-optical signal processing [6], or perfect absorbers in solar photovoltaic and stealth applications [7]. For plasmonic antennas, the generally low Q factors make it possible to choose any frequency within a broad bandwidth of resonances while still ensuring strong field enhancement thanks to small mode volumes [8]. Unfortunately, significant light absorption in metals (Ohmic losses) introduces severe restrictions in many applications, especially in the emerging optical signal processing regime [6]. A search for alternative approaches using all-dielectric nanostructures supporting Mie resonances is, therefore, becoming essential [9]. To deal with large radiation losses associated with typical Mie resonances, researchers started exploiting the concept of a bound state in the continuum (BIC) [10] and its derivative, a quasi-BIC (QBIC) [11]. First proposed in quantum mechanics, this concept has expanded rapidly into a new field that has continued to grow exponentially after its introduction into photonics [12–16].

Guided modes (GMs) in photonic structures, e.g., in a slab waveguide, are known to have continuous dispersion curves over a broad frequency range below the light cone. Such modes boast infinite-quality factors, and they are therefore inaccessible from the far field. Several works in the literature have discussed the intrinsic connection between GMs and conventional guided resonances [17,18]. When the momentum mismatch between the GMs and the incident plane waves is compensated for by introducing some geometrical perturbations to form periodic structures, leaky modes in the continuum will be formed. These modes are known as guided mode resonances (GMRs) [19], and they occur at the second-order stop band [20]. The Q factors of the GMRs deteriorate significantly in most regions of the k-space

*chengwei.qiu@nus.edu.sg
†zhan@sdnu.edu.cn

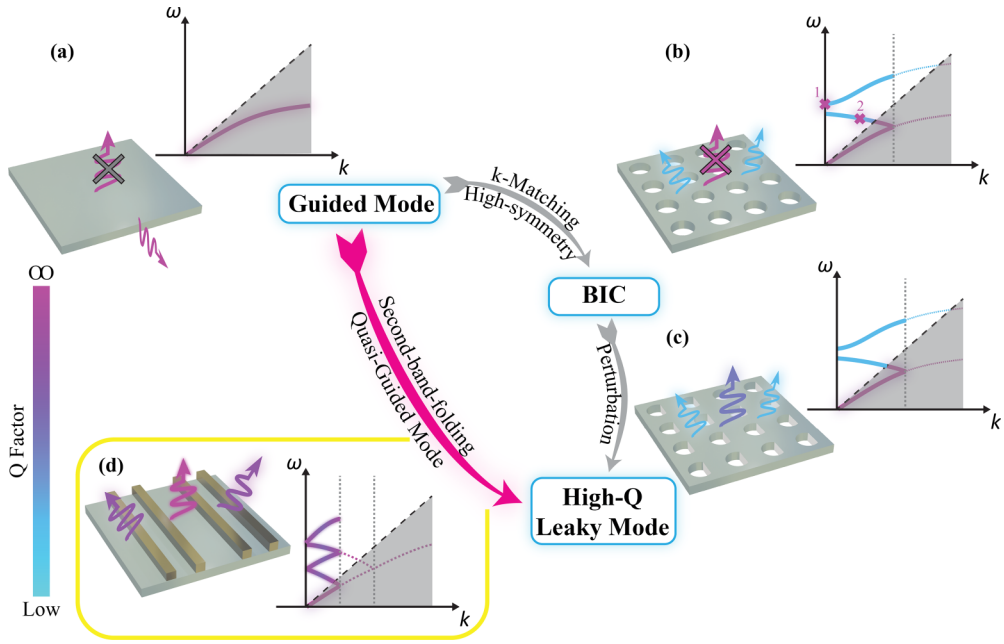

FIG. 1. Conceptual diagram for generating high-Q leaky modes, illustrating the differences between the traditional and proposed approaches. The slab waveguide in (a) is first periodically perturbed to produce GMRs above the light cone as in (b). High-Q modes are only retained at discrete points, known as symmetry-protected (marker 1) and accidental (marker 2) BICs. Disturbing the unit cells breaks the symmetry and leads to quasi-BICs in (c). Although radiations are allowed, the frequencies at these points are restricted within a narrow bandwidth dependent on the perturbation. The proposed double-band-folding strategy, as shown in (d), omits the intermediate BIC stage and moves GMs directly into the light cone, thereby preserving ultrahigh Q factors over the same spectral band as the GMs.

except at a few discrete points with high symmetry, where the infinite-Q factors of the original GMs are retained, forming a BIC point. Typical instances of high symmetry include the Γ point with perfectly antisymmetric mode profiles, and the case in which two radiation channels have the same coupling coefficient amplitudes and opposite phases, which correspond to the symmetry-protected and accidental types of BIC, respectively [10]. The latter case is often accompanied by the behavior of avoided crossing, which is not shown in Fig. 1 for simplicity. This is the origin of BIC supported by many periodic structures, e.g., resonant gratings on slab waveguides [21], photonic crystal slabs [22], and metasurfaces [11]. Another equivalent approach to explain the requirement of high symmetry in BIC resonances is based on their topological nature [23]. BICs may form at the singularity points of vortex centers in the polarization directions of far-field radiation, where the polarization is undefined. However, regardless of the approaches considered previously, the BIC can only occur at very few discrete points in the k-space, which can be considered zero-dimensional (0D) resonances. In contrast, the original GMs have infinite-Q factors over the whole operation bandwidth. This outstanding feature cannot be applied to BICs through conventional interpretations. When certain perturbations are introduced into the photonic systems, the original BIC resonances are disturbed into QBIC, which are possible for free-propagating wave excitation but lose their infinite-Q factors [24,25]. Although this is currently a popular and dominant approach for achieving leaky modes with high Q factors through wavelength-scale or even subwavelength-size optical nanostructures, the main drawback is that the frequency of the resulting QBIC resonance is located within a narrow spectral band close to that of the original BIC, even at a wave number highly different from that of the BIC point in the k-space. This band is even narrower when one aspires to a higher Q factor at a weaker perturbation. This narrowband limitation of QBIC resonances poses significant restrictions in many applications, where light-matter interactions need to be enhanced in broad spectral ranges. To address this limitation, various approaches have been exploited, e.g., using an elaborate geometrical design to merge several BICs at distinct locations in the k-space so that their corresponding QBIC operation bands overlap [26], or using degenerate BICs to have more robustness of the Q-factor relative to the perturbations [27]. However, the number of merged BICs is usually limited, and the overall bandwidth, over which one can realize high Q factor resonances, is still rather narrow. New concepts, including lines of BICs [28] or a ring of BICs [29], have also been explored. However, these approaches require the involvement of axially symmetric structures such as two-dimensional photonic crystals with the third dimension infinitely long [30] or a sphere array, which are challenging to implement in practical applications. Besides, the wave vectors providing infinite-Q factors are still limited to a finite set, and the availability over a broad frequency bandwidth still needs more investigation.

Here, we first realize an effective manipulation method that truly converts guided modes below the light cone to radiative modes above the light cone in periodic structures. From the relations between GMs, BICs, QBICs, and radiations, as illustrated by Fig. 1, we propose in this work a strategy to realize leaky resonances by transforming the GMs into leaky QGMs (quasi-GMs) with ultrahigh Q factors

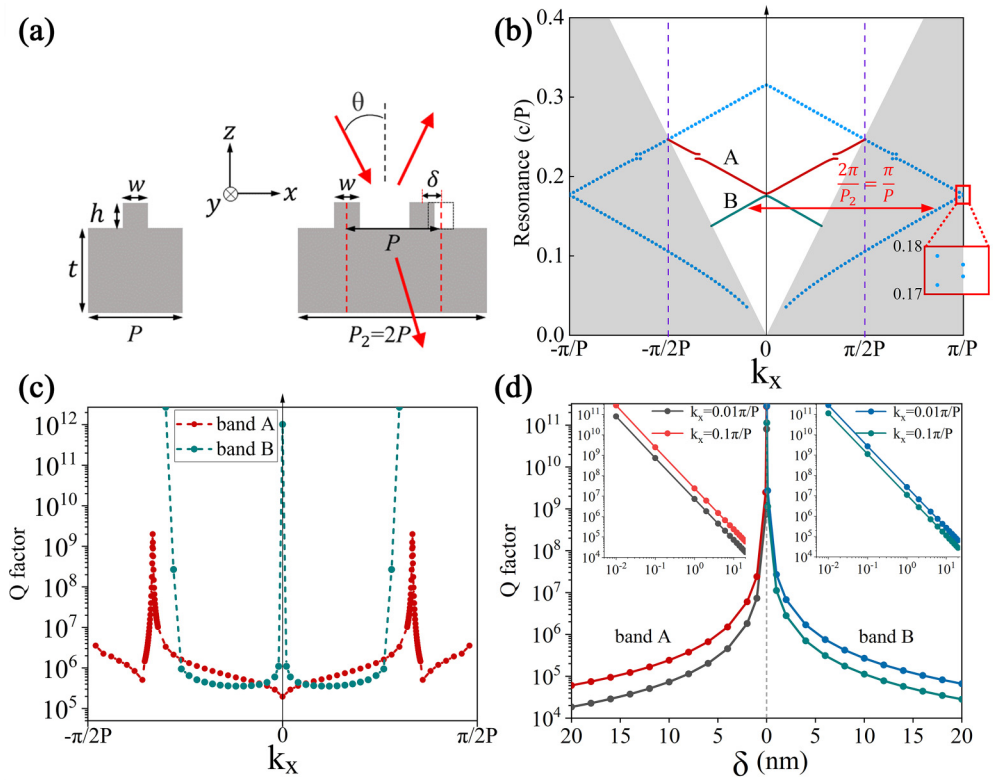

FIG. 2. (a) Schematics of a regular grating (left) and a compound grating (right) consisting of two ridges on a slab waveguide. The compound grating is formed by shifting the lateral position of every second ridge, leading to a new period of $2P$. (b) Dispersion curves for modes supported by both the two-ridge compound grating (solid lines) and the undistorted one-ridge grating (blue dashed lines). The following geometrical parameters are used: $P = 540$ nm, $t = 220$ nm, $h = 60$ nm, $w = 50$ nm, and $\delta = 5$ nm. The inset is an enlargement of the spectral gap at the boundary of the FBZ. (c) Calculated Q factors for the QGMs supported by the compound grating; (d) Q factor vs the lateral shift δ for four arbitrary points, two on each band.

directly. Since the intermediate process of BIC is not necessary and thus can be circumvented, it is now possible to achieve novel leaky modes over a broad bandwidth. Consequently, the problem with the narrowband operation in the general BIC effect supported by periodic structures will be properly addressed. The transition from the GMs into QGMs is achieved when a perturbation is introduced between adjacent unit cells of a regular periodic structure to distort the photonic lattice and increase the periodicity by an integer of times. We do note that a similar dimerized grating structure has been investigated in the literature [31]. However, the connection between realized high-Q resonances and guided modes was not noticed, as the focus was still put on discrete BIC points but not on the GMs. As a result, the first Brillouin zone (FBZ) of the original GMs will be folded. Due to the translational symmetry in the k-space, the dispersion curves of GMs originally extending to the FBZ boundary of the undistorted lattice will be folded above the light cone, denoting the occurrence of leaky resonances. When the perturbation is weak, the leaky resonances will retain many properties of the original GMs while keeping ultrahigh Q factors, which are strongly dependent on the level of perturbation, in a similar manner to the QBIC resonance [11]. If the GMs supported by the original undistorted structure have strong spatial dispersions (i.e., steep dispersion curves) over a broad bandwidth in the k-space, the same behavior will also be found in the new leaky modes. Thus, it is possible to spectrally tune the resonance or even excite multiple resonances simultaneously by simply choosing the proper incident angles. As a result, enhanced interactions between matter and light at different wavelengths or multiple wavelengths simultaneously can be easily achieved.

We next use a 1D ridge grating on a slab waveguide to demonstrate the basic idea of achieving QGMs. As schematically shown in Fig. 2(a), both the ridges and the waveguide slab are assumed to be in the air and made from silicon (index 3.45). Without losing generality, the TE-polarization is considered with the electric field parallel to the y-direction and the incident beam within the xz-plane at an angle of θ with respect to the normal of the surface. The commercial software COMSOL MULTIPHYSICS, which is based on the finite-element method (FEM), is used for all the calculations, adopting the lateral Floquet periodic boundary conditions to account for the wave number k_x. A regular grating structure on a slab waveguide periodically modulates the propagation of the guided modes and provides a momentum of $K_0 = 2\pi/P$ (P is the grating period), giving rise to a coupling between two counterpropagating guided modes [32]. This coupling is manifested by the appearance of a spectral gap at the FBZ boundary, $k_x = \pm\pi/P$, which is also known as the first-order stopband. However, when the lattice is perturbatively distorted by shifting the lateral position of every second ridge

by δ, a compound grating composed of two alternatingly aligned ridge arrays with a doubled period of $P_2 = 2P$ will be formed. Similar lattice distortion can also be achieved by changing the ridge width, e.g., compound gratings exploited in the literature to improve the angular tolerance of narrow band filters [20]. Due to the translational symmetry in the k-space with a period of $2\pi/P_2 = \pi/P$, the QGMs will possess the dispersion relation $f(k_x) = f(k_x + \pi/P)$.When the perturbation is weak, the distorted lattice will exhibit resonances similar to those supported by the undistorted lattice, i.e., $f(k_x + \frac{\pi}{P}) \approx f_0(k_x + \frac{\pi}{P})$, where $f_0(k_x)$ is the dispersion of the GMs. Consequently, $f(k_x) \approx f_0(k_x + \pi/P)$, which implies that the dispersion curves of the GMs in the undistorted lattice centered at $k_x = \pm\pi/P$ will appear around $k_x = 0$, leading to the occurrence of a new set of leaky modes at the first stopband (in contrast with GMRs, which occur at the second stopband) with the dispersion curves flipped from below the light cone to above it.

Figure 2(b) presents the calculated band structure from eigenfrequency analysis for the QGMs supported by the compound grating when δ is 5 nm. The dispersion curves for the GMs supported by the original undistorted one-ridge grating are also presented as the dashed blue lines, which extend to the boundary of the FBZ of the one-ridge grating at $k_x = \pm\pi/P$. A small spectral gap can be seen at the FBZ boundary [see the inset of Fig. 2(b)], which is due to the small ridges and the weak modulation of the refractive index of the slab [32]. In the folded dispersion curves of the GMs, two identical small spectral gaps (one on each side) are found at the frequency around $0.222c/P$ (c is the vacuum light speed), which are attributed to the coupling between two copropagating guided modes in the Si slab and the photonic lattice layer, respectively [33]. For a nonzero value of δ, it is clear from Fig. 2(b) that the same dispersion profiles of two crossed dispersion curves from the GMs can be found in the QGMs supported by the compound grating, although the dispersion curves for the two cases have been shifted by a value of $2\pi/P_2$. The avoided crossing behaviors at the frequency of $0.222c/P$ are also shown, which turn out to be accidental BICs [see the infinite-Q factors at the crossing in Fig. 2(c)]. Since we are only interested in the leaky resonances for light-matter interactions, only the resonances above the light lines are presented for the compound grating. The extension of dispersion curves beyond the light line is not shown because they correspond to GMs in that case, with infinite-Q factors and no coupling to free-space radiations.

We plot in Fig. 2(c) the calculated Q factors for the QGMs presented in Fig. 2(b). Both bands exhibit ultrahigh Q factors over large bandwidths with different evolution trends as the wave number increases. For the low-frequency branch (band B), the resonance at the Γ point corresponds to an ideal symmetry-protected BIC and thereby has an infinite-Q factor. This arises from a mirror symmetry in the compound grating across the central plane between two adjacent ridges, regardless of the value of δ. Resonances along the high-frequency branch (band A) first see a slight increase in the Q factor until they reach the accidental BIC point, which originates from the coupling between two copropagating guided modes [19]. The Q factor surges to infinity at this point, followed by a sudden drop and a subsequent increase again for wave numbers beyond. When both branches extend beyond the cross with the light line, the Q factors will be infinite because the resonances under the light line are essentially GMs. Clearly, the well-known BIC concepts still enter the discussion as the overall structure has a periodicity of $2P$. The difference is that the resonances with ultrahigh Q factors are now observable over the entire first Brillouin zone, unlike their BIC counterparts, which are discrete. The reason is that those resonances are originally the guided modes of the grating with a periodicity of P. A perturbation with doubled periodicity effectively shrinks the first Brillouin zone, exposing those modes in regions above the light cone.

One distinctive behavior for all the QGMs in Fig. 2(b) is that the Q factors have a significant dependence on the level of perturbation. To demonstrate this point, in Fig. 2(d) we plot the calculated Q factors at two different wave numbers on each band. All the results exhibit the same inversely quadratic dependence of Q factors on the lateral shift δ of every second ridge, and the Q factors surge to infinity as δ vanishes. This behavior is very similar to the QBIC resonances, which are generated by introducing some geometrical perturbation into a metasurface structure supporting BIC [11]. When δ vanishes for the QBIC resonances, their dispersion curve shrinks to a point corresponding to the original BIC; however, the QGMs will switch back to GMs with the profile of the dispersion curve unchanged. In other words, the Q factors of all the QGMs on the two bands in Fig. 2(b) can be tuned to infinity. This is valid for any frequency over the large operation bandwidth, significantly outperforming BICs which can only occur at a few discrete frequencies. A tuning of the resonance wavelength by changing the incident angle and the huge local electric field enhancement on resonance can be seen from the results provided in the supplemental material [34].

The idea of transforming GMs into QGMs with lattice distortion can be extended to more general cases with the new period $P_m = mP$, where m is an integer denoting the number of periods in the original structure to be unified into the new unit cell. To achieve leaky modes, one should ensure that the dispersion curves of the GMs by the undistorted lattice will appear above the light cone after a few translational operations along the k_x axis, i.e., $|k_x - jk_m| < k_0$, where $k_x \in (k_0,\ \pi/P]$ and k_0 are the wave numbers of the original GM and light in free space at the same frequency, respectively, $j \in (0,\ m)$ is an integer, $k_m = 2\pi/P_m$ is the momentum provided by the compound grating, and it can be controlled by the number of ridges involved. As a subsequent example, we use a three-ridge compound grating structure shown in the inset of Fig. 3(b) to demonstrate the generality. Instead of shifting the position of the ridges, we switch to an alternative approach of increasing the width of every second (third) ridge by an increment of $\delta = 5$ nm compared to the first (second) one. After the lattice distortion, the period of the compound grating becomes $P_3 = 3P$. The momentum from this new grating will be reduced to $2\pi/P_3$, leading to the folding of the original guided modes at $k_x = \pm\pi/P$ to $k_x = \pm\pi/3P$. Figure 3(a) presents the calculated band structure of the QGMs by the new grating. Compared to the case of a two-ridge grating, multiple bands appear within the FBZ in the wave-number range of $(-\pi/P_3,\ \pi/P_3)$ leading to more foldings of the

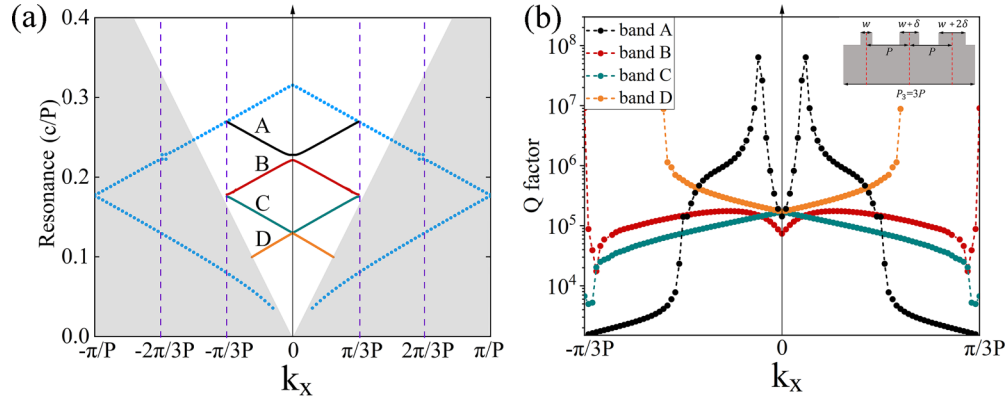

FIG. 3. (a) Dispersion curves for both the three-ridge compound grating (solid lines) and the unperturbed one-ridge grating (blue dashed lines). (b) The Q factors for the leaky resonances supported by the three-ridge compound grating. The schematic of a compound grating composed of three ridges on a slab waveguide is shown in the inset.

dispersion. The original anticrossing behaviors located at the frequency $0.222c/P$ and wave numbers around $k_x = \pm 2\pi/P_3$ appear as a spectral gap between branches A and B around the Γ point. The Q factors for the resonances along these bands are plotted in Fig. 3(b). There is no symmetry-protected BIC resonance for the three-ridge compound grating, which exhibits no mirror symmetry. However, the two Q factor peaks at two small k_x on band A correspond to two accidental BICs. Furthermore, we note the high dependence of the Q factors for all the resonances on the level of perturbation, and the trend of Q approaching infinity for a zero δ, as shown in Fig. 2(d), persists for the three-ridge compound grating.

Although the simple 1D periodic structure of compound ridge gratings on a slab waveguide is used above to demonstrate the transition from GMs to QGMs, we note that the slab waveguide is not essential and the same physics can be easily extended to other periodic gratings or more general metasurfaces (see the supplemental material [34] for examples). One typical example is the zigzag array of dielectric disks schematically shown in Fig. 4(a), which has been widely employed in QBIC applications [35]. For simplicity, we use a special case in which $P_{2x} = 2P_y$ so that when the relative angle α between two disks vanishes, the whole structure becomes a photonic crystal slab (PCS) structure of the rod-type composed of Ge (index 4.01) disks aligned in the square lattice on a CaF_2 (index 1.38) substrate. This PCS is known to support GMs [36], whose dispersion curve is calculated and presented by the dotted lines in Fig. 4(b). When a nonzero α is introduced, a compound double-disk structure of the zigzag array is formed with the period in the x-direction increasing from P_x to P_{2x}, and the FBZ shrinks in the k_x axis; see the inset of Fig. 4(b). The GMs will switch to QGMs with the dispersion curves at the X point of FBZ in the square lattice, $f_0(k_x + \pi/P_x,\ k_y)$, folded to $f(k_x,\ k_y)$ in the zigzag array. As a result, a strong dependence of QGM resonance on the incident angle for the TM_x mode in the x-direction and the TE_y mode in the y-direction can be observed [20]. The calculated dispersion curves of the QGMs are presented as the solid lines in Fig. 4(b), confirming the connection between the QGMs and GMs. We further plot in Fig. 4(c) the dependence of the Q factors on the relative angle α at two arbitrary wave numbers $k = 0.02\pi/P_x$ and $0.12\pi/P_x$ along both lateral directions on the dispersion curve in Fig. 4(b). Similar to the case of compound grating structure, the Q factors exhibit a strong dependence on the geometry perturbation and approach infinity when α vanishes. Further studies also confirm that this dependence of the Q factor and the trend of it to infinity is true for any wave number, supporting the origination of QGMs from GMs.

The results shown by the simulations provide a promising way to realize QGMs experimentally. One can use mature material platforms such as a silicon-on-insulator or Ge on the CaF_2 substrate, whose processing techniques have been fully developed, for photonic applications. One can even use different ridge materials from the slab waveguide in Fig. 2 so that the slab layer does not need to be patterned.

In conclusion, we have unveiled in this work a strategy to generate an alternative type of leaky resonances by transforming the GMs with broadband infinite-Q factors directly into QGMs, without resorting to the use of BICs. While the collective behaviors between resonating elements have been explored for high Q factor photonic structures including phase gradient metasurfaces [37] and beam splitters [38], we have reported a unified relation between GMs, QGMs, BICs, QBICs, and radiations. In general, these QGMs combine all the advantages (including ultrahigh Q factors, huge local electric enhancement, and intermediate mode volume) from various photonic resonators, such as photonic crystal cavities [3], whispering-gallery modes [4], plasmonic nanoantennas [8], and QBIC resonances [10]. They further represent a significant advancement over the BIC effect in many aspects, particularly when considering the bandwidth over which ultrahigh Q factors are available. The strategy to generate leaky resonances based on lattice distortion, although conceptually simple, can provide a completely new and ideal platform for light-matter interactions based on all-dielectric structures, with broad application potentials in a large variety of optical fields. For example, broadband operations can significantly boost nonlinear applications with multiple inputs tuned on resonance simultaneously, which is not possible with the QBIC effect.

This work has been supported by the National Science Foundation of China under Grants No. 11974221 and

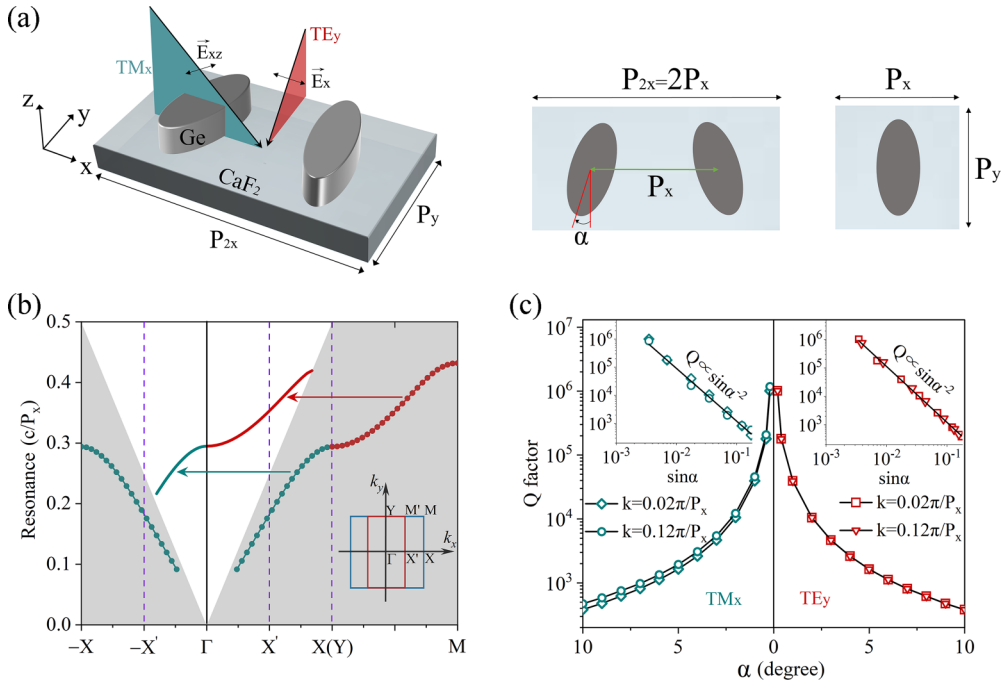

FIG. 4. (a) (left) Schematic diagram of the incident light. (right) Primitive cells of the periodic structure for two different cases: (1) both disks are rotated from the symmetry axis by an angle; (2) a single disk with no rotation. Other parameters include $P_x = P_y = 2.34\ \mu$m; the long and short axis of the disks are 2.25 and 0.9 μm, respectively. (b) Dispersion curves calculated for the two cases in (a) with α being 10°. (c) Dependence of the resonance Q factors on the relative angle of α at two different wave numbers.

No. 12274269. Z.H. also thanks Sergey I. Bozhevolnyi at the University of Southern Denmark and Yuri Kivshar at Australian National University for fruitful inputs.

[1] T. J. Seok, A. Jamshidi, M. Kim, S. Dhuey, A. Lakhani, H. Choo, P. J. Schuck, S. Cabrini, A. M. Schwartzberg, J. Bokor, E. Yablonovitch, and M. C. Wu, Radiation engineering of optical antennas for maximum field enhancement, Nano Lett. **11**, 2606 (2011).

[2] E. M. Purcell, Spontaneous emission probabilities at radio frequencies, in *Confined Electrons and Photons*, edited by E. Burstein and C. Weisbuch (Springer, Boston, 1995), Vol. 340, pp. 839–839.

[3] Y. Akahane, T. Asano, B.-S. Song, and S. Noda, High-Q photonic nanocavity in a two-dimensional photonic crystal, Nature (London) **425**, 944 (2003).

[4] G. Lin, A. Coillet, and Y. K. Chembo, Nonlinear photonics with High-Q whispering-gallery-mode resonators, Adv. Opt. Photon. **9**, 828 (2017).

[5] G. New, *Introduction to Nonlinear Optics* (Cambridge University Press, Cambridge, 2011).

[6] A. E. Willner, S. Khaleghi, M. R. Chitgarha, and O. F. Yilmaz, All-optical signal processing, J. Light. Technol. **32**, 660 (2014).

[7] Y. D. Chong, L. Ge, H. Cao, and A. D. Stone, Coherent Perfect Absorbers: Time-Reversed Lasers, Phys. Rev. Lett. **105**, 053901 (2010).

[8] M. Kauranen and A. V. Zayats, Nonlinear plasmonics, Nat. Photon. **6**, 737 (2012).

[9] S. Kruk and Y. Kivshar, Functional meta-optics and nanophotonics governed by mie resonances, ACS Photon. **4**, 2638 (2017).

[10] C. W. Hsu, B. Zhen, A. D. Stone, J. D. Joannopoulos, and M. Soljačić, Bound states in the continuum, Nat. Rev. Mater. **1**, 16048 (2016).

[11] K. Koshelev, S. Lepeshov, M. Liu, A. Bogdanov, and Y. Kivshar, Asymmetric Metasurfaces with High-Q Resonances Governed by Bound States in the Continuum, Phys. Rev. Lett. **121**, 193903 (2018).

[12] E. N. Bulgakov and A. F. Sadreev, Bound states in the continuum in photonic waveguides inspired by defects, Phys. Rev. B **78**, 075105 (2008).

[13] Y. Plotnik, O. Peleg, F. Dreisow, M. Heinrich, S. Nolte, A. Szameit, and M. Segev, Experimental Observation of Optical Bound States in the Continuum, Phys. Rev. Lett. **107**, 183901 (2011).

[14] C. W. Hsu, B. Zhen, J. Lee, S. L. Chua, S. G. Johnson, J. D. Joannopoulos, and M. Soljačić, Observation of trapped light within the radiation continuum, Nature (London) **499**, 188 (2013).

[15] Y. Yang, C. Peng, Y. Liang, Z. Li, and S. Noda, Analytical Perspective for Bound States in the Continuum in Photonic Crystal Slabs, Phys. Rev. Lett. **113**, 037401 (2014).

[16] D. C. Marinica, A. G. Borisov, and S. V. Shabanov, Bound States in the Continuum in Photonics, Phys. Rev. Lett. **100**, 183902 (2008).

[17] V. N. Astratov, I. S. Culshaw, R. M. Stevenson, D. M. Whittaker, M. S. Skolnick, T. F. Krauss, and R. M. De La Rue,

Resonant coupling of near-infrared radiation to photonic band structure waveguides, J. Light. Technol. **17**, 2050 (1999).

[18] S. G. Tikhodeev, A. L. Yablonskii, E. A. Muljarov, N. A. Gippius, and T. Ishihara, Quasiguided modes and optical properties of photonic crystal slabs, Phys. Rev. B **66**, 045102 (2002).

[19] G. Quaranta, G. Basset, O. J. F. Martin, and B. Gallinet, Recent advances in resonant waveguide gratings, Laser Photon. Rev. **12**, 1800017 (2018).

[20] F. Lemarchand, A. Sentenac, and H. Giovannini, Increasing the angular tolerance of resonant grating filters with doubly periodic structures, Opt. Lett. **23**, 1149 (1998).

[21] D. A. Bykov, E. A. Bezus, and L. L. Doskolovich, Coupled-wave formalism for bound states in the continuum in guided-mode resonant gratings, Phys. Rev. A **99**, 063805 (2019).

[22] A. Kodigala, T. Lepetit, Q. Gu, B. Bahari, Y. Fainman, and B. Kanté, Lasing action from photonic bound states in continuum, Nature (London) **541**, 196 (2017).

[23] B. Zhen, C. W. Hsu, L. Lu, A. D. Stone, and M. Soljačić, Topological Nature of Optical Bound States in the Continuum, Phys. Rev. Lett. **113**, 257401 (2014).

[24] Z. Han, F. Ding, Y. Cai, and U. Levy, Significantly enhanced second-harmonic generations with all-dielectric antenna array working in the quasi-bound states in the continuum and excited by linearly polarized plane waves, Nanophotonics **10**, 1189 (2021).

[25] Meta-optics and bound states in the continuum, Sci. Bull. **64**, 836 (2019).

[26] M. Kang, S. Zhang, M. Xiao, and H. Xu, Merging Bound States in the Continuum at Off-High Symmetry Points, Phys. Rev. Lett. **126**, 117402 (2021).

[27] A. Sadreev, E. Bulgakov, A. Pilipchuk, A. Miroshnichenko, and L. Huang, Degenerate bound states in the continuum in square and triangular open acoustic resonators, Phys. Rev. B **106**, 085404 (2022).

[28] A. Cerjan, C. W. Hsu, and M. C. Rechtsman, Bound States in the Continuum Through Environmental Design, Phys. Rev. Lett. **123**, 023902 (2019).

[29] A. S. Kostyukov, V. S. Gerasimov, A. E. Ershov, and E. N. Bulgakov, Ring of bound states in the continuum in the reciprocal space of a monolayer of high-contrast dielectric spheres, Phys. Rev. B **105**, 075404 (2022).

[30] A. Cerjan, C. Jorg, S. Vaidya, S. Augustine, W. A. Benalcazar, C. W. Hsu, G. Von Freymann, and M. C. Rechtsman, Observation of bound states in the continuum embedded in symmetry bandgaps, Sci. Adv. **7**, 3 (2021).

[31] A. C. Overvig, S. Shrestha, and N. Yu, Dimerized high contrast gratings, Nanophotonics **7**, 1157 (2018).

[32] R. Kazarinov and C. Henry, Second-order distributed feedback lasers with mode selection provided by first-order radiation losses, IEEE J. Quantum Electron. **21**, 144 (1985).

[33] S.-G. Lee, S.-H. Kim, and C.-S. Kee, Bound states in the continuum (bic) accompanied by avoided crossings in leaky-mode photonic lattices, Nanophotonics **9**, 4373 (2020).

[34] Supplemental Material at http://link.aps.org/supplemental/10.1103/PhysRevB.107.115415 for a demonstration of resonance wavelength tunability, the local field enhancement effect, and several other applicable metasurface examples.

[35] A. Leitis, A. Tittl, M. Liu, B. H. Lee, M. B. Gu, Y. S. Kivshar, and H. Altug, Angle-multiplexed all-dielectric metasurfaces for broadband molecular fingerprint retrieval, Sci. Adv. **5**, 1 (2019).

[36] S. G. Johnson, S. Fan, P. R. Villeneuve, J. D. Joannopoulos, and L. A. Kolodziejski, Guided modes in photonic crystal slabs, Phys. Rev. B **60**, 5751 (1999).

[37] A. C. Overvig, S. C. Malek, and N. Yu, Multifunctional Nonlocal Metasurfaces, Phys. Rev. Lett. **125**, 017402 (2020).

[38] M. Lawrence, D. R. Barton, J. Dixon, J.-H. Song, J. van de Groep, M. L. Brongersma, and J. A. Dionne, High quality factor phase gradient metasurfaces, Nat. Nanotechnol. **15**, 956 (2020).